Princeton University

Optimal Nonlinear Estimation for Aircraft Flight Control in Wind Shear

Sandeep S. Mulgund
Department of Mechanical and Aerospace Engineering
Princeton University

JUP Quarterly Review
April 1-2, 1993
Princeton, NJ

Laboratory for Control and Automation

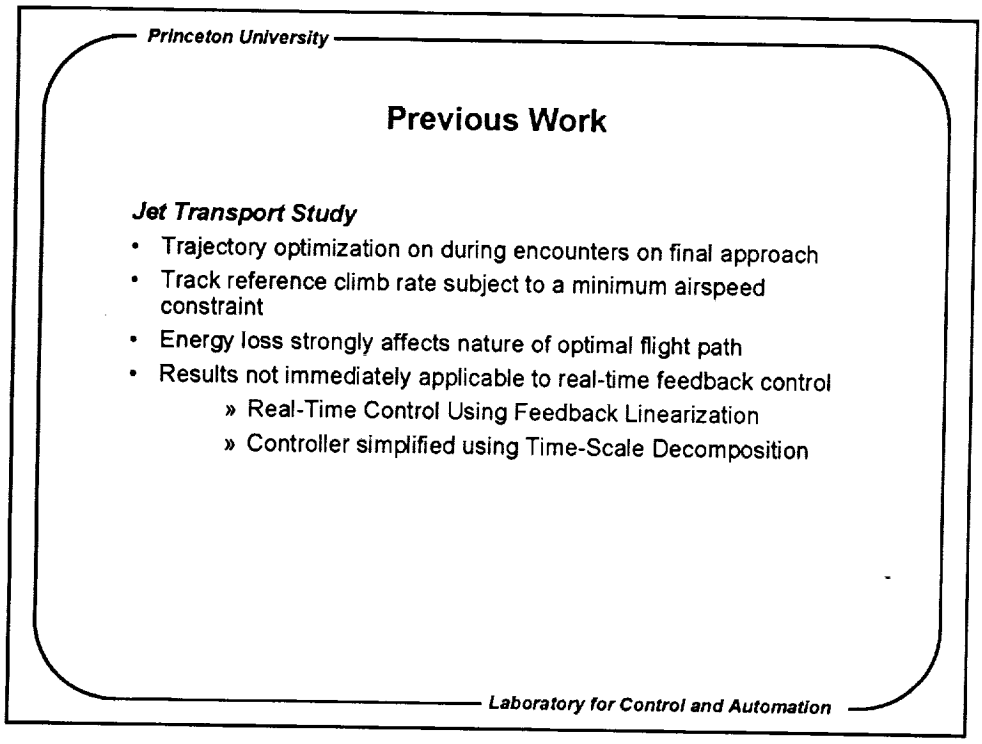

This presentation describes the most recent results in an ongoing research effort at Princeton in the area of flight dynamics in wind shear. The first undertaking in this project was a trajectory optimization study. The flight path of a medium-haul twin-jet transport aircraft was optimized during microburst encounters on final approach. The assumed goal was to track a reference climb rate during an aborted landing, subject to a minimum airspeed constraint. The results demonstrated that the energy loss through the microburst significantly affected the qualitative nature of the optimal flight path. In microbursts of light to moderate strength, the aircraft was able to track the reference climb rate successfully. In severe microbursts, the minimum airspeed constraint in the optimization forced the aircraft to settle on a climb rate smaller than the target. A tradeoff was forced between the objectives of flight path tracking and stall prevention.

Although the results provided a qualitative picture of the nature of an optimal control strategy in wind shear, they were not immediately applicable to real-time control. Optimization is an iterative process requiring global knowledge of the flow field. Therefore, an initiative was undertaken to develop feedback control methods that approximated the performance realized in the optimal trajectories. The technique of nonlinear inverse dynamics or feedback linearization was used to develop a control law for a nonlinear model of the aircraft dynamics. The control design was simplified using *Time-Scale Decomposition,* which permitted the partitioning of the controller into a slow outer loop and a fast inner loop.

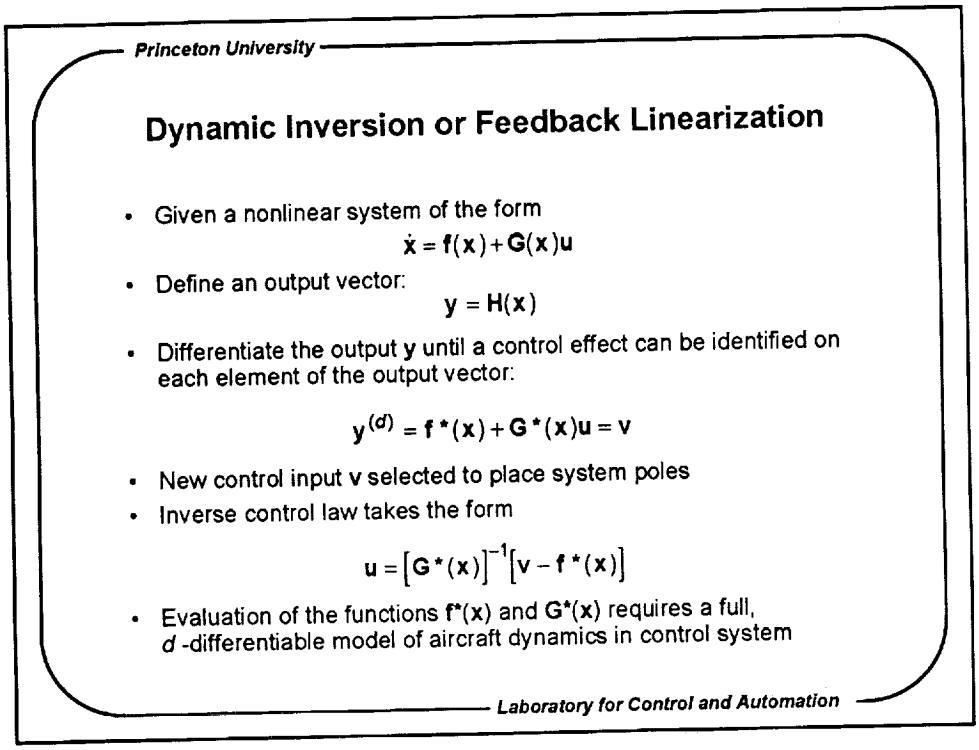

The control law designed for the aircraft model was based on the technique of dynamic inversion or feedback linearization. Given a nonlinear system of the form shown, it is possible to define an output vector **y** which is a known function of the system state **x**. This output is differentiated with respect to time until a control effect can be identified on each element of the output vector. The d^{th} derivative of the output is then equated to a new control input **v**. This control input can be selected to place the system poles in designer-specified locations, subject to the controllability of the original system. Although the form of the resultant nonlinear control law appears simple, the evaluation of its components requires that a full, d-differentiable model of the plant dynamics be included in the control system.

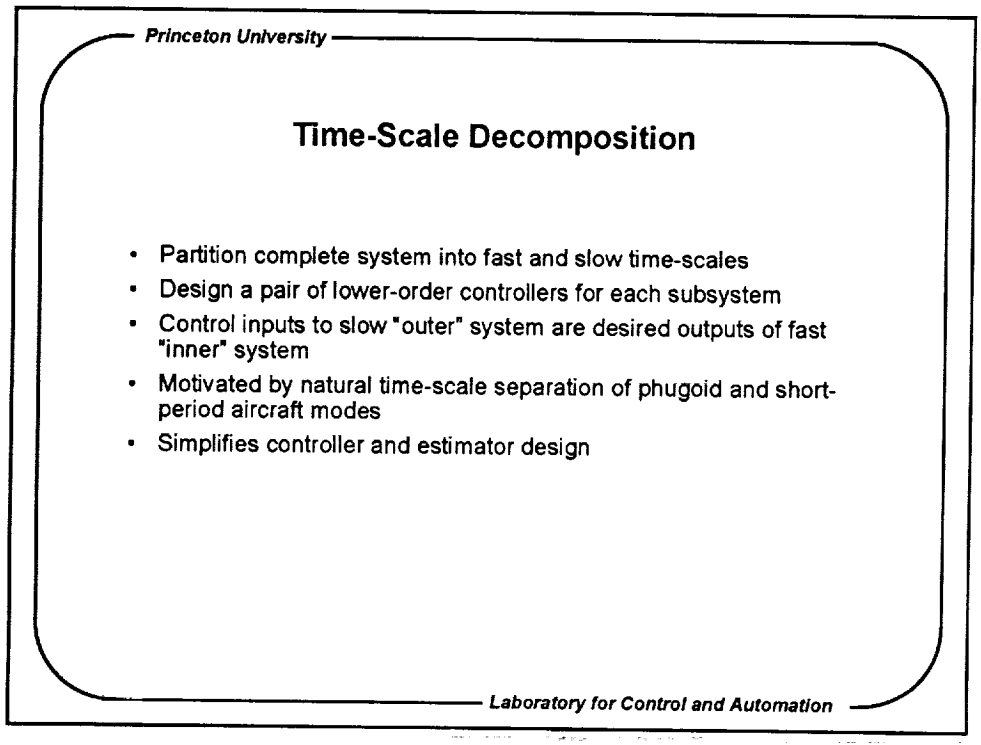

The control law based on nonlinear inverse dynamics can be simplified if it is possible to partition the original system into fast and slow time scales. If this is feasible, it is possible to design a pair of lower-order controllers for each subsystem. The control inputs to the slow "outer" system are the desired outputs of the fast "inner" system. For the aircraft problem, the time-scale decomposition is motivated by the time-scale separation that exists between the phugoid and short-period modes. The application of this technique simplifies both the controller and estimator design. Two lower-order controllers can be designed, and fewer system state derivatives must be estimated.

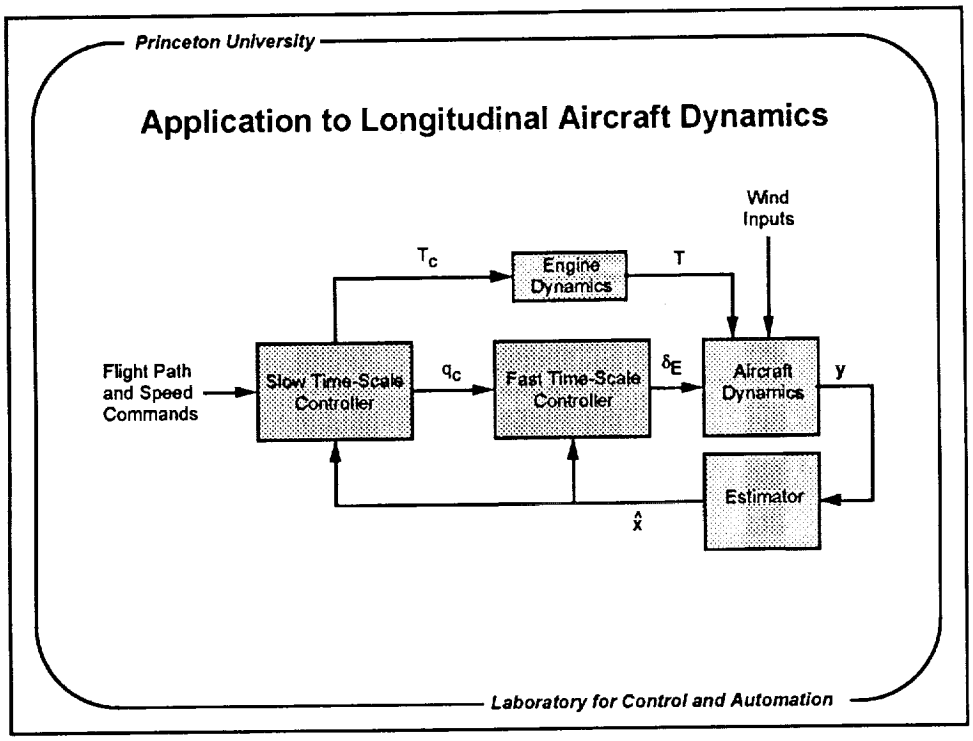

The structure of the nonlinear control law using time-scale decomposition is illustrated here for our aircraft study. The slow outer controller accepts flight path and speed commands. It generates a throttle and pitch rate command. The throttle command is passed on to the engine dynamics. The pitch rate command becomes the desired response of the fast inner controller. This controller generates the elevator deflection required to achieve the desired pitch rate. This controller is designed to have a response time at least 3 to 5 times faster than the outer controller. Thus from the perspective of the outer controller, the necessary pitch rate is achieved almost instantaneously. The elevator deflection calculated by the fast controller is fed into the aircraft dynamics, as is the actual thrust level produced by the engine dynamics. The output of the aircraft sensors is fed into an estimator, which generates the aircraft state estimate needed to accomplish the inversion. The design of this estimator and the performance of the controller/estimator pair are the subject of the rest of this presentation.

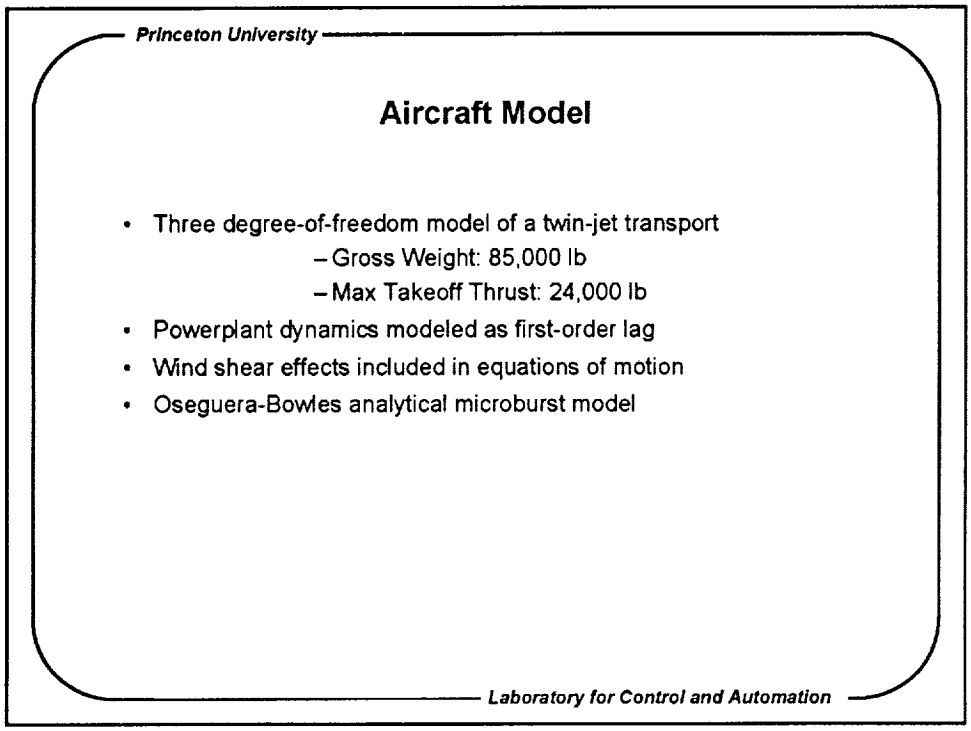

A three degree-of-freedom model of a twin-jet transport aircraft was used for this study. The aircraft has the given gross weight and maximum takeoff thrust. The powerplant dynamics are modeled as a first-order lag, and thrust lapse with mach number and altitude is also modeled. Wind shear effects are incorporated into the equations of motion, and the Oseguera-Bowles microburst model (developed at NASA Langley Research Center) provides the wind inputs used in simulated microburst encounters.

Princeton University

Control Strategies in Microburst Wind Shear

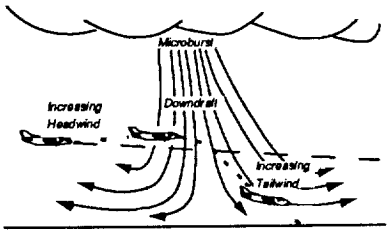

Airspeed Control

- Undesirable thrust reduction in headwind region
- Maintains airspeed in tailwind

Groundspeed Control

- Maintains thrust in headwind region
- Airspeed loss in tailwind

Laboratory for Control and Automation

The control law described earlier is designed to track reference speed and flight path inputs. It is worthwhile to consider what types of guidance strategies are suitable in a microburst environment. In a classical microburst encounter, the aircraft first encounters an increasing headwind. The airspeed increases, and the aircraft may balloon above the nominal flight path. If the flight crew is not alert to the fact that a microburst is present, they may take action to prevent the plane from climbing by throttling back and/or lowering the aircraft's nose. This headwind soon transitions to a downdraft, which may result in an increased sink rate. The subsequent tailwind causes an airspeed loss, and ground impact may result if the pilot does not apply an effective recovery technique.

Regulating airspeed about a nominal value causes an undesirable reduction in thrust in the headwind region of the shear to prevent an unwanted airspeed increase. This may leave the aircraft in a precarious state once it enters the performance-decreasing downdraft and tailwind. However, airspeed is maintained in the tailwind region, subject to the powerplant performance limits. Conversely, regulation of groundspeed maintains thrust in the headwind region. A thrust increase is typically required in the headwind region to maintain a nominal groundspeed. In the tailwind region, however, groundspeed regulation results in an airspeed loss and may lead to stall if the airspeed becomes too low. Taken together, these observations suggest that an effective strategy might be one that combines the desirable traits of groundspeed and airspeed control.

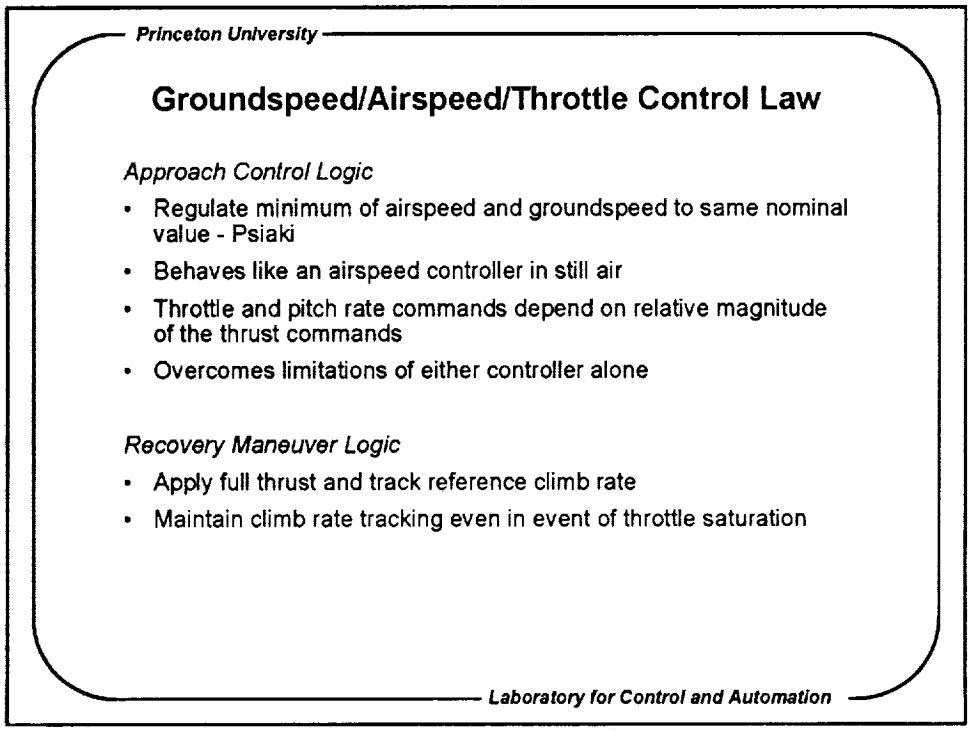

The guidance strategy used with the nonlinear control law was adapted from one developed by Mark Psiaki of Cornell University. The approach control logic regulates the minimum of airspeed and groundspeed to the same nominal value. This behaves like an airspeed controller in still air. In the current implementation, the throttle and pitch rate commands passed onto the aircraft dynamics depend on the relative magnitudes of the thrust commands generated by an airspeed/climb rate and a groundspeed/climb rate controller. This control logic overcomes the limitations of either airspeed or groundspeed control alone. During a recovery maneuver (where a decision is made to abort an approach and execute an escape trajectory), full thrust is applied directly together with a climb rate command.

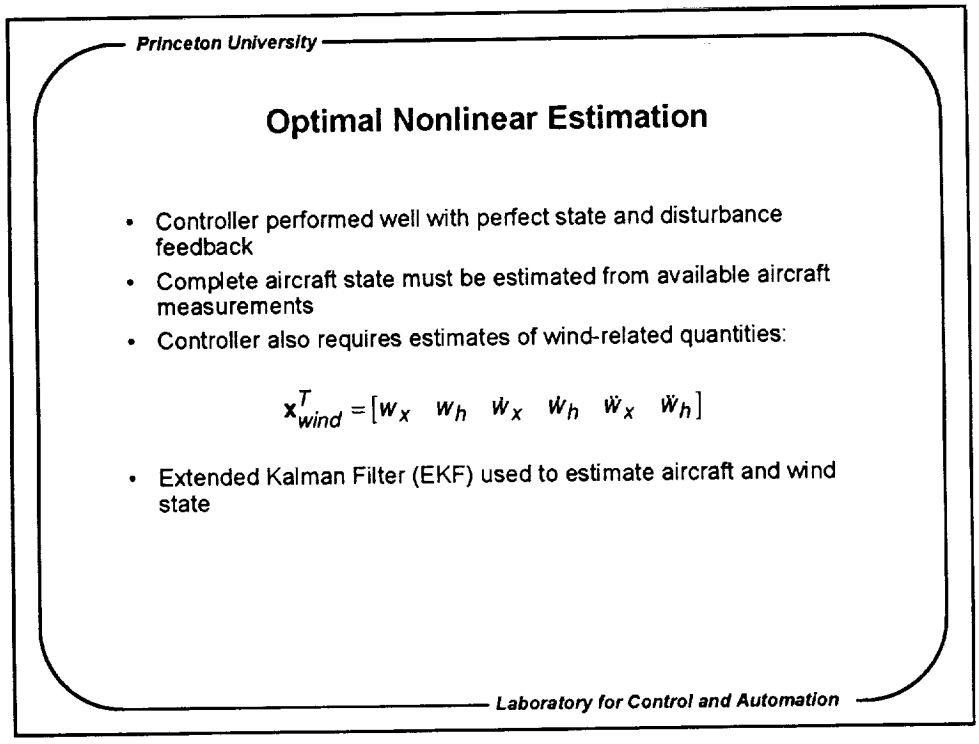

The control logic described earlier was found to perform well with perfect aircraft and wind state feedback. The time-scale separation assumption was demonstrated to be valid, and the controller provided good recovery performance in a broad spectrum of microbursts. In practice, however, the complete aircraft state must be estimated from the available air-data and inertial measurements. The controller also requires feedback of the two wind components (horizontal and vertical) together with their first and second time-derivatives. The *Extended Kalman Filter* (EKF) was postulated as a candidate estimator structure for this problem.

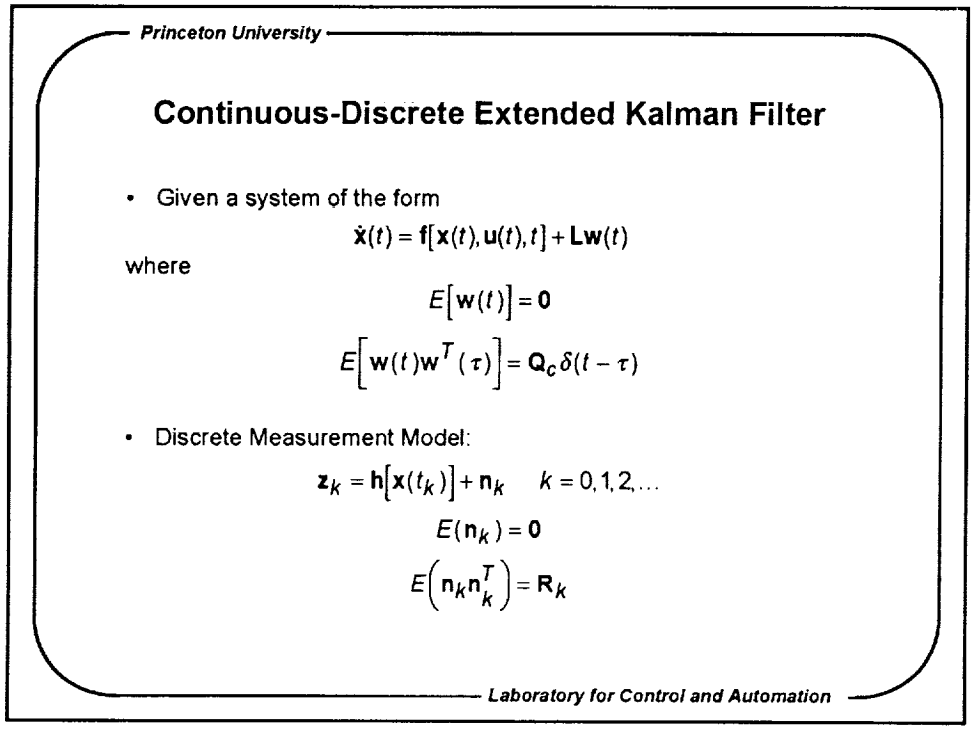

This form of the EKF is based upon a continuous model of plant dynamics and a discrete measurement model. The disturbance $\mathbf{w}(t)$ influencing the plant dynamics is assumed to be a zero-mean Gaussian white noise process with a known spectral density matrix $\mathbf{Q}$. The measurements $\mathbf{z}_k$ are made at discrete instances t_k, and are known functions of the plant state. The measurement noise vector $\mathbf{n}_k$ is assumed to be a zero-mean Gaussian white noise process with known covariance $\mathbf{R}$.

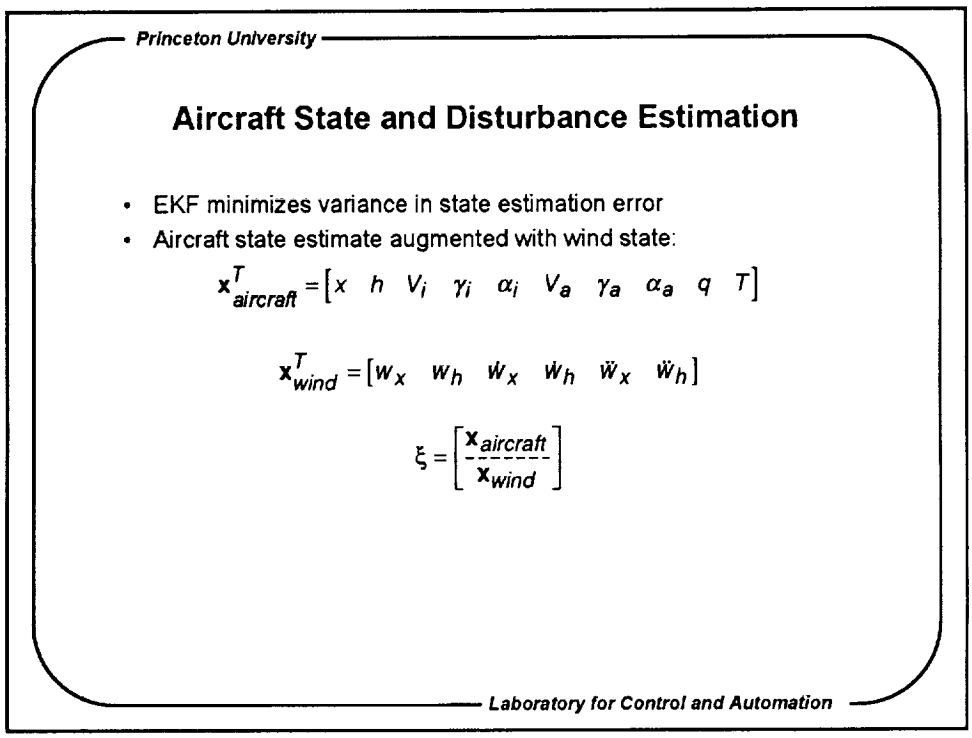

The form of the EKF for the aircraft problem is now described. The nonlinear control law requires feedback of the wind state in addition to that of the aircraft state. This is achieved by defining the system state to consist of the aircraft and wind state. The wind state is defined to be the horizontal and vertical wind components, together with their first two time-derivatives.

Princeton University

Complete System Equations

- Wind dynamics:

$$\begin{bmatrix} \dot{w}_x \\ \dot{w}_h \\ \ddot{w}_x \\ \ddot{w}_h \\ \dddot{w}_x \\ \dddot{w}_h \end{bmatrix} = \begin{bmatrix} 0 & 0 & 1 & 0 & 0 & 0 \\ 0 & 0 & 0 & 1 & 0 & 0 \\ 0 & 0 & 0 & 0 & 1 & 0 \\ 0 & 0 & 0 & 0 & 0 & 1 \\ 0 & 0 & 0 & 0 & 0 & 0 \\ 0 & 0 & 0 & 0 & 0 & 0 \end{bmatrix} \begin{bmatrix} w_x \\ w_h \\ \dot{w}_x \\ \dot{w}_h \\ \ddot{w}_x \\ \ddot{w}_h \end{bmatrix} + \begin{bmatrix} 0 & 0 \\ 0 & 0 \\ 0 & 0 \\ 0 & 0 \\ 1 & 0 \\ 0 & 1 \end{bmatrix} \begin{bmatrix} w_1 \\ w_2 \end{bmatrix}$$

$$\dot{\mathbf{x}}_{wind} = \mathbf{F}_{wind}\mathbf{x}_{wind} + \mathbf{L}_{wind}\mathbf{w}$$

- Aircraft Dynamics:

$$\dot{\mathbf{x}}_{aircraft} = \mathbf{f}(\mathbf{x}_{aircraft}, \mathbf{x}_{wind}, \mathbf{u})$$

- Complete System Equations:

$$\dot{\xi} = \begin{bmatrix} \dot{\mathbf{x}}_{aircraft} \\ \hline \dot{\mathbf{x}}_{wind} \end{bmatrix} = \begin{bmatrix} \mathbf{f}(\mathbf{x}_{aircraft}, \mathbf{x}_{wind}, \mathbf{u}) \\ \mathbf{F}_{wind}\mathbf{x}_{wind} \end{bmatrix} + \begin{bmatrix} \mathbf{0} \\ \mathbf{L}_{wind} \end{bmatrix} \mathbf{w}$$

Laboratory for Control and Automation

The wind dynamics are modeled as a linear system driven by an external input **w**. The components of **w** are thus the third time-derivatives of w_x and w_h. The complete system equations shown here become the basis of the Kalman filter equations presented earlier.

Princeton University

Simulation Examples

- Measurements:

$$\mathbf{z}^T = \left[h \;\; V_i \;\; V_a \;\; \alpha_a \;\; \theta \;\; q \;\; \dot{h} \;\; \ddot{x} \;\; \ddot{h}\right]$$

$$\mathbf{R_o} = diag\left(5,\ 4,\ 4,\ 0.025^2,\ 0.025^2,\ 0.025^2,\ 2,\ 2,\ 2\right)$$

- Sensor noise statistics based on conservative estimates of expected accuracy

Case Number	Simulation Parameters	Measurement and Control Model
1	NID only	$\mathbf{u} = \mathbf{g}(\mathbf{x})$
2	NID and EKF; Perfect measurements	$\mathbf{u} = \mathbf{g}(\hat{\mathbf{x}})$ $\mathbf{z} = \mathbf{h}(\mathbf{x}) \Leftrightarrow \mathbf{R} \approx \mathbf{0}$
3	NID and EKF; Noisy measurements	$\mathbf{u} = \mathbf{g}(\hat{\mathbf{x}})$ $\mathbf{z} = \mathbf{h}(\mathbf{x}) + \mathbf{n}$

Laboratory for Control and Automation

A set of nine measurements were postulated for the simulation examples. The assumed sensors were altitude, groundspeed, airspeed, angle of attack, pitch attitude and rate, climb rate, and horizontal and vertical acceleration. The sensor noise statistics were based on conservative estimates of the expected accuracy of those sensors. Three simulations were conducted using the same initial conditions and microburst wind profile. The simulations were structured in such a way to illustrate the degradation in controller performance caused by removing the assumption of perfect state feedback. In the first case, the NID controller was driven by perfect state feedback. In the second and third cases, the controller was driven by the output of an EKF that utilized the measurement vector shown. The difference between Cases 2 and 3 was that in Case 2, there was no noise in the sensor measurements. The performance realized here would thus be indicative of the theoretical limit of the performance of the NID/EKF combination. In Case 3, the measurements were noisy and had the statistics indicated by the matrix $\mathbf{R}_o$.

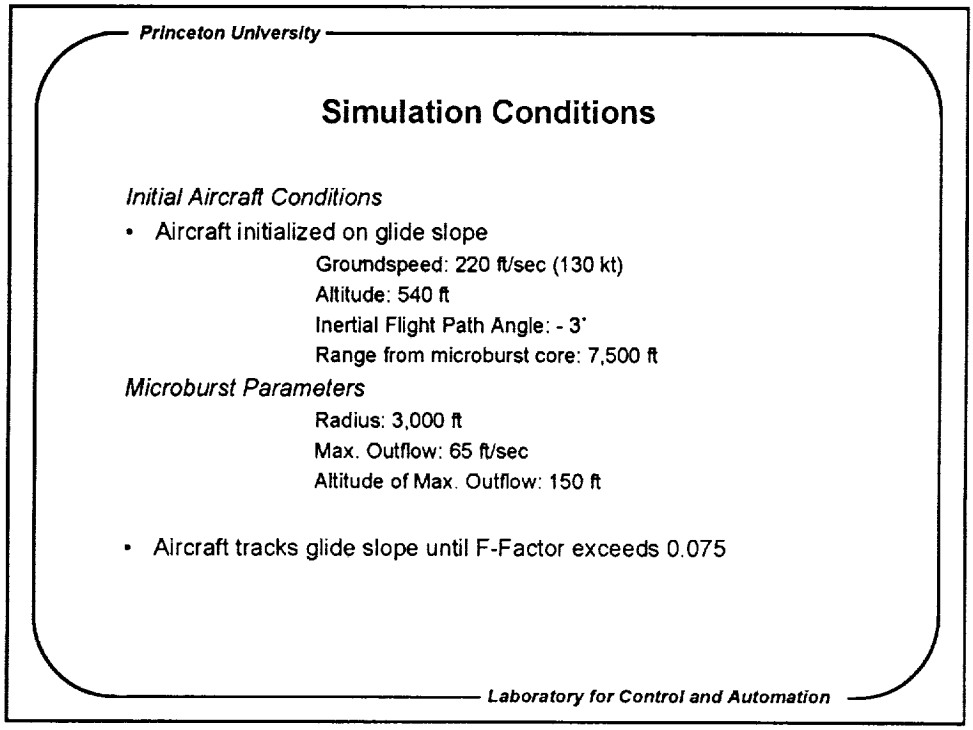

In all of the simulations conducted, the same initial conditions and microburst parameters were used. The aircraft was placed in an approach configuration a fixed distance away from the microburst core. The aircraft tracked the glide slope until the F-Factor exceeded a preset threshold, at which point a recovery was commanded using full thrust and a nominal climb rate of 5 ft/sec. For Cases 2 and 3 where the EKF was in use, the recovery was triggered on the basis of an estimate of the F-Factor.

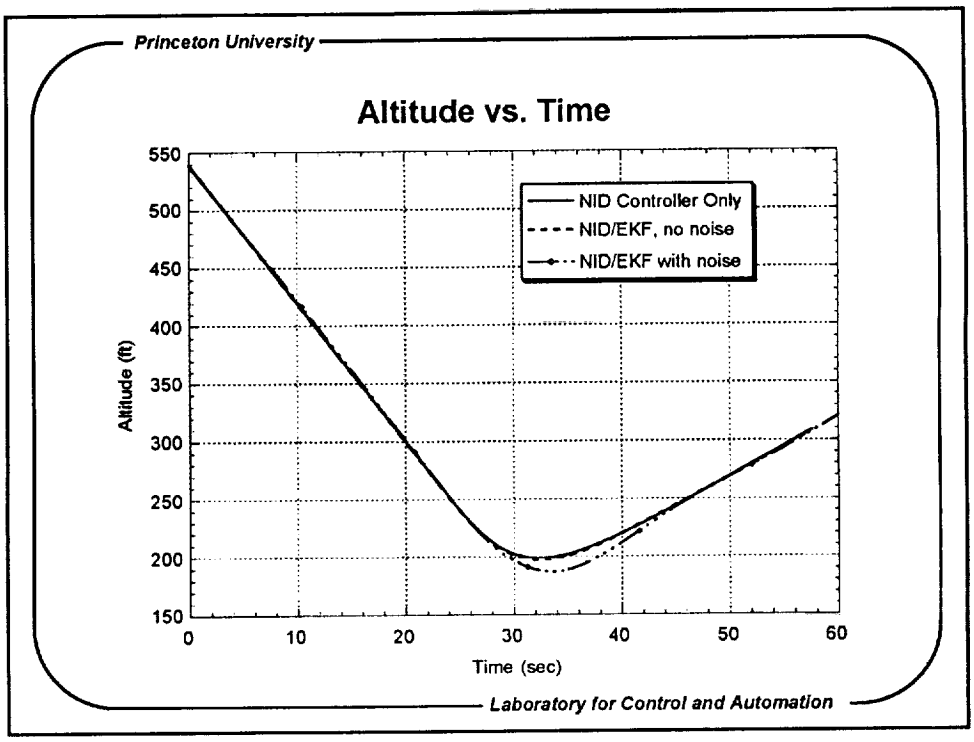

The altitude time-histories are shown here for the three simulation examples. It is apparent that there is little to no controller performance degradation between Cases 1 and 2. This suggests that in the limit as aircraft sensors become more and more accurate, the baseline performance realized using perfect state feedback can be achieved. There is only a slight loss in performance in Case 3, where the controller is driven by state estimates derived from noisy measurements.

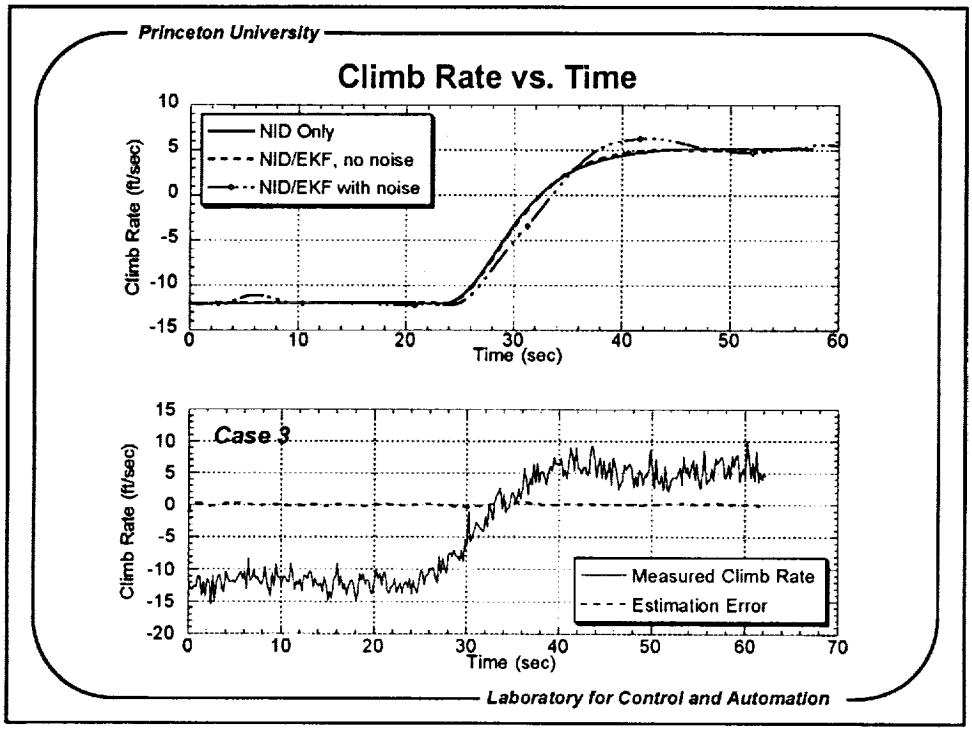

The climb rate histories for the 3 cases are shown in the top figure. Those from Cases 1 and 2 are quite similar to one another. In Case 3, there is more overshoot in the response of the aircraft. The performance of the EKF is indicated in the bottom figure. The output of the climb rate sensor is shown for Case 3, together with the resultant estimation error in climb rate. The magnitude of the estimation error is much smaller than the apparent level of noise in the sensor output. This indicates that the EKF is effective in eliminating the effects of measurement noise in the estimation of climb rate.

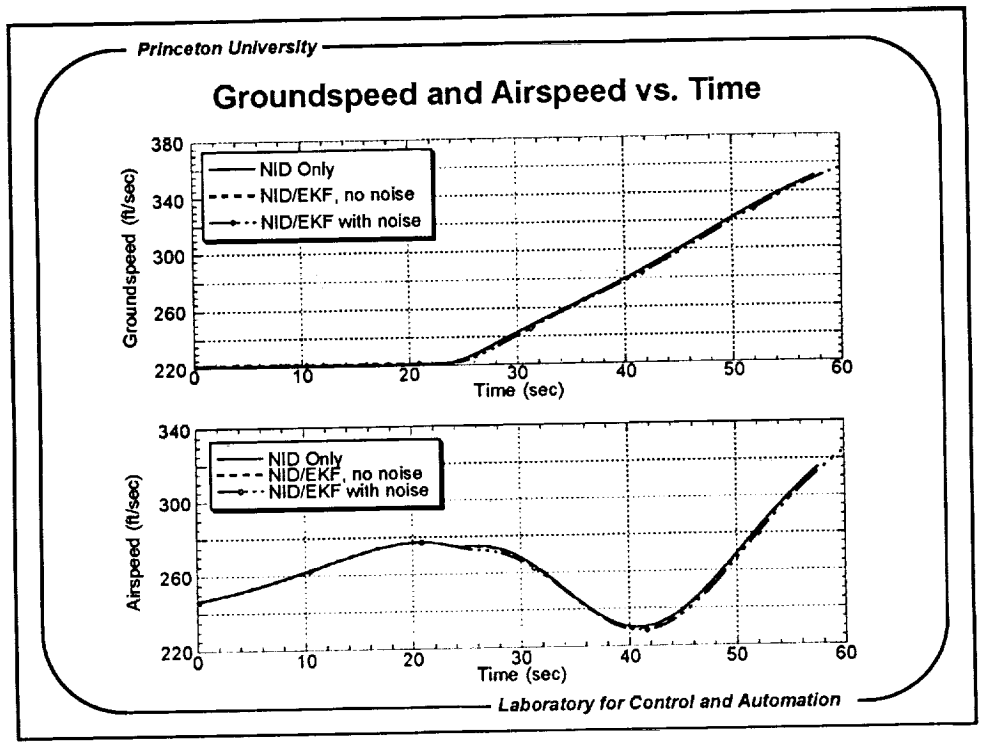

Groundspeed and airspeed climb rate histories are shown here for all three cases. They are virtually identical to one another. In the approach portion of the trajectory, the aircraft is able to track the reference groundspeed extremely well even when driven by optimal estimates derived from noisy measurements of groundspeed.

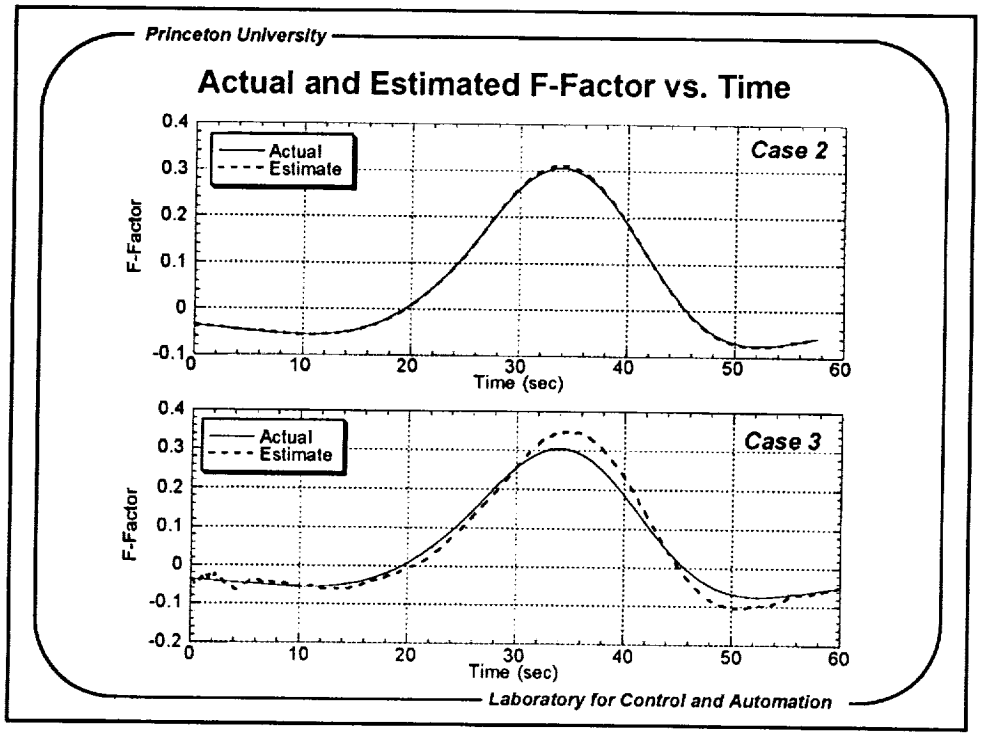

The ability of the EKF to estimate the F-Factor hazard index is illustrated here for Cases 2 and 3. In Case 2 where the EKF uses perfect measurements, the F-Factor is estimated very accurately. When noisy measurements are introduced in Case 3, some estimation lag becomes noticeable in the EKF output. The F-Factor estimates seem to lag the most when the sign of the F-Factor's time-derivative changes sign. The peak F-Factor is actually overpredicted by the EKF.

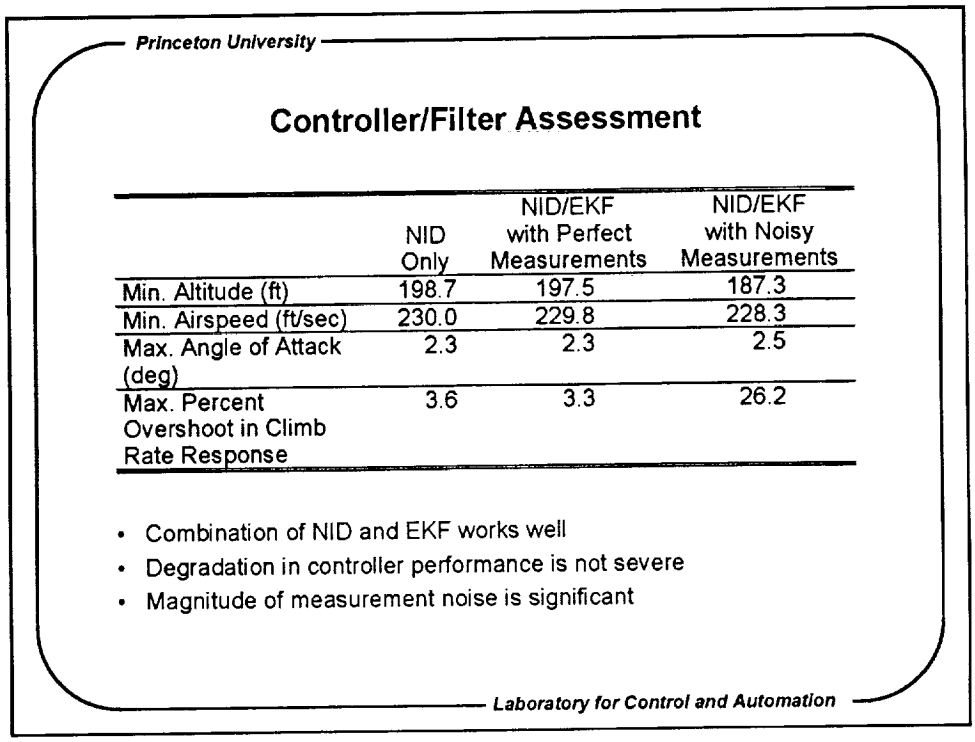

A summary is provided here of some salient features of each of the three cases. The difference in minimum altitude between Cases 1 and 3 is only 10.4 ft. The minimum airspeed is only 2 knots lower in Case 3 as compared to Case 1. This would suggest that in terms of maintaining safety margins, the EKF/NID combination is almost as effective as the NID alone driven by perfect state feedback. There is almost no difference in maximum angle of attack as well. The principal difference between Cases 1 and 3 is in the climb rate response of the aircraft. In Case 3, there is much more response overshoot than in Case 1. This is likely due to filter lags arising from uncertainty in the accuracy of the measurement vector.

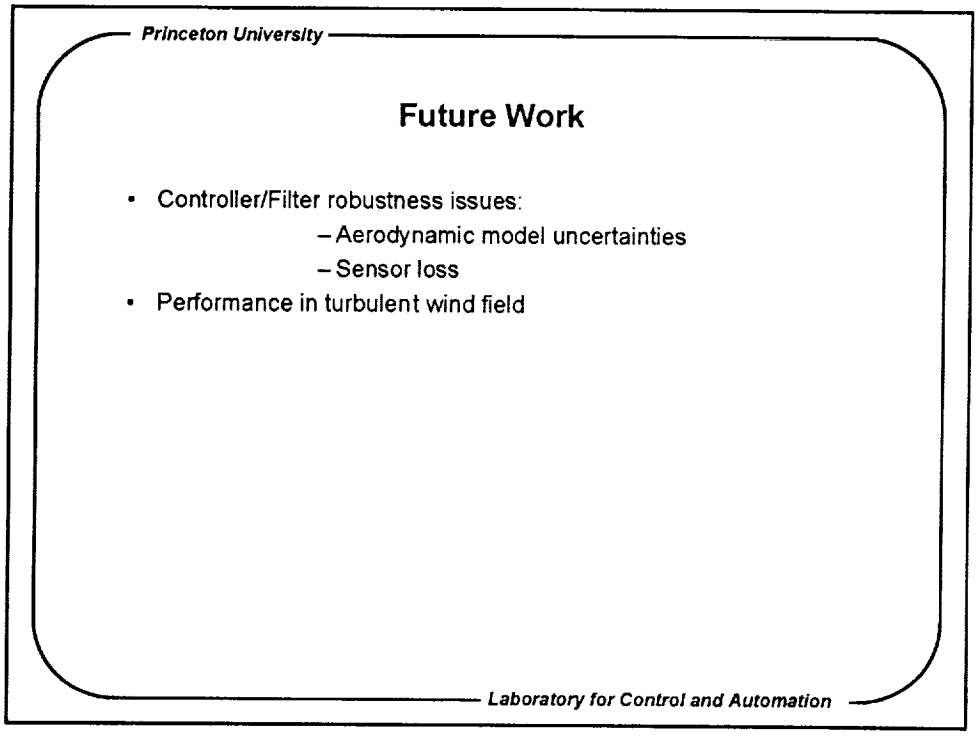

There are a number of unresolved issues to be addressed in this work. The robustness of the NID/EKF combination to aerodynamic modelling errors will be studied. The system performance with a reduced sensor suite will also be investigated. The ability of the controller to track flight path command through a turbulent wind field will be investigated. It may be necessary to tune the EKF parameters to reduce unwanted control activity in wind fields containing high-frequency components.